




Genome-wide association study of rice (*Oryza sativa* L.) inflorescence architecture

Masoumeh Kordi^a, Naser Farrokhi^{a,1,*}, Asadollah Ahmadikhah^{a,2,*}, Pär K. Ingvarsson^{b,3,*} , Abbas Saidi^a, Mehdi Jahanfar^a

^a Department of Cell & Molecular Biology, Faculty of Life Sciences & Biotechnology, Shahid Beheshti University, Tehran, Iran

^b Department of Plant Biology, Swedish University of Agricultural Sciences, Uppsala, Sweden

ARTICLE INFO

Keywords:

Epistasis
Haplotype analysis
GWAS
Population structure
Protein-protein interaction network analyses
QTLs
RNA-seq data analysis

ABSTRACT

Rice yield strongly depends on panicle size and architecture but the genetics underlying these traits and their coordination with environmental cues through various signaling pathways have remained elusive. A genome-wide association study (GWAS) was performed to pinpoint the underlying genetic determinants for rice panicle architecture by analyzing 20 panicle-related traits using a data set consisting of 44,100 SNPs. We defined QTL windows around significant SNPs by the rate of LD decay for each chromosome and used these windows to identify putative candidate genes associated with the trait. Using a publicly available RNA-seq data set we performed analyses to identify the differentially expressed genes between stem and panicle with putative functions in panicle architecture. In total, 52 significant SNPs were identified, corresponding to 41 unique QTLs across the 12 rice chromosomes, with the most signals appearing on chromosome 1 (nine associated SNPs), and seven significant SNPs for each of chromosomes 8 and 12. Some novel genes such as *Ankyrin*, *Duf*, *Kinesin* and *Brassinosteroid insensitive* were found to be associated with panicle size. A haplotype analysis showed that genetic variation in haplotypes qMIL2 and qNSBBH21 were related to two traits, MIL, the greatest distance between two nodes on the rachis, and NSBBH, the number of primary branches in the bottom half of a panicle, respectively. Analysis of epistatic interactions revealed a marker affecting clustered traits. Several QTLs were identified on different chromosomes for the first time which may explain the phenotypic diversity of rice panicle architecture we observe in our collection of accessions. The identified candidate genes and haplotypes could be used in marker-assisted selection to improve rice yield through gene pyramiding.

1. Introduction

The green revolution in the mid-20th century resulted from an architectural change in rice from low to dense panicles (Pasion et al., 2021; Batool et al., 2023; Singh et al., 2024) and panicle architecture

hence plays an important role in controlling rice yield (Ntakirutimana et al., 2023). Inflorescence development occurs in three stages: (Li et al., 2020) the transition of the shoot apical meristem (SAM) to an inflorescence meristem (IM), (Zhuang et al., 2020) the production of several primary branch meristems (PBMs), and (Pasion et al., 2021) the

Abbreviation: QTL, quantitative trait locus; GWAS, genome-wide association study; SNP, single nucleotide polymorphism; RNA-seq, RNA sequencing; LD, Linkage disequilibrium decay; ACC, Accessions; PPI, protein-protein interaction; SAM, shoot apical meristem; IM, inflorescence meristem; PBM, primary branch meristems; ABA, abscisic acid; BR, brassinosteroids; TEJ, temperate japonica; IND, indica; ARO, aromatic; TRJ, tropical japonica; P-TRAP, Panicle TRAIT Phenotyping; RGB image, Red, Green, and Blue; H2_b, Broad-sense heritability; OMAP project, Oryza Map Alignment Project; MLM, mixed linear models; FarmCPU, fixed and random model circulating probability unification; GLM, general linear model; PC, principal components; QQplot, quantile-quantile plot; FPKM, fragments per kb per million reads; DEG, differentially expressed gene; GO, Gene Ontology; DUF, Domains of unknown function; Kip, Cyclin Inhibitory Protein/Kinase inhibitory protein; MF, molecular function; BP, biological process; CC, cellular component; PC, protein class; NB-ARC, nucleotide-binding adaptor shared by APAF-1, R proteins, and CED-4; Dof, DNA-binding with one finger; LRR-LRK, Leucine-rich repeat receptor-like kinase; KRPs, Kip-related proteins.

* Corresponding authors.

E-mail addresses: n_farrokhi@sbu.ac.ir (N. Farrokhi), a_ahmadikhah@sbu.ac.ir (A. Ahmadikhah), par.ingvarsson@slu.se (P.K. Ingvarsson).

¹ ORCID: 0000-0003-4676-1545

² ORCID: 0000-0001-5100-9740

³ ORCID: 0000-0001-9225-7521

<https://doi.org/10.1016/j.plantsci.2024.112382>

Received 28 October 2024; Received in revised form 13 December 2024; Accepted 30 December 2024

Available online 9 January 2025

0168-9452/© 2025 The Author(s). Published by Elsevier B.V. This is an open access article under the CC BY license (<http://creativecommons.org/licenses/by/4.0/>).

formation of subsequent species-specific branching that leads to the final inflorescence architecture (Fig. 1a). These developmental stages have major effects on rice grain number and hence ultimately on crop yield. The rice inflorescence (Fig. 2) consists of a main axis in the middle with primary, secondary, and higher-order branches (Bai et al., 2021a; Li et al., 2021a). In rice, the process of panicle development and the panicle branching pattern is highly dependent on the timing of inflorescence meristem abortion, the conversion of the rachis branch meristem to terminal spikelet meristem, and the formation of lateral spikelets (Pasion et al., 2021; Zhu et al., 2022). High-yielding rice cultivars produce longer primary and more secondary branches than low-yielding genotypes (Ntakirutimana et al., 2023; Agata et al., 2020). Panicle or inflorescence branching in rice is under strong genetic control with high heritability ($H^2 = 75\text{--}84\%$) (Bai et al., 2021a) but is also influenced by hormonal and environmental factors (Bai et al., 2021a; Harrop et al., 2019). Environmental factors such as temperature (Weng et al., 2014), water (Du et al., 2018), light (Xie et al., 2019), nutrition (Wang et al., 2021), and pathogens and insects (Sun et al., 2020) have all been shown to be important in influencing rice panicle architecture.

Effects of hormonal cross-talk in defining inflorescence architecture of rice has also been reported and the roles of cytokinins (cell division and floral organ growth and development; (Han et al., 2014)), auxins (initiation and maintenance of the axillary meristem affecting inflorescence branching; 18), and gibberellins (organ elongation, seed germination, and flowering) are all well established. Nevertheless, the role of other hormones such as ethylene, abscisic acid (ABA), and brassinosteroids should not be ignored (Chun et al., 2022; Wu et al., 2016). GAs oppose cytokinins in maintaining SAM activity (Shi and Vernoux, 2019). These positive and negative effects of hormones sometimes fail to revert effects on the panicle phenotype caused by other hormones (Chun et al., 2022). Receptor histidine kinases, histidine phosphotransfer proteins (Yao et al., 2023), cytokinin oxidase/dehydrogenase and response regulators convey the cytokinin signal transduction (Duan et al., 2019a) and this signaling cascade results in the definition of panicle length (Duan et al., 2019a), branch, spikelet, and seed numbers (Rong et al., 2024). The GIBBERELLIN INSENSITIVE DWARF1 (GID1) receptor and the cytochrome P450 monooxygenase gene *OsCYP71D8L* have been shown to play substantive roles in mediating the effects of GA signaling on panicle size and architecture (Ueguchi-Tanaka et al., 2005). Also, ABA content is positively correlated with the potential of

grain-filling in rice (*Oryza sativa* L.) cultivars when comparing the inferior (late-flowering) vs. the superior (early-flowering) spikelets (Zhang et al., 2012a).

GWAS is a reliable technique for dissecting the genetic control of plant traits and have successfully been employed to identify loci controlling wheat grain yield (Li et al., 2019), plant architecture (Muhammad et al., 2021) and flag leaf morphology (Li et al., 2021a). In rice, GWAS has previously been used to dissect the genetic architecture of the main features of panicle morphology using 162 *Oryza glaberrima* Steud accessions, identifying several genes related to panicle architecture, including *OgPHYB* (Ntakirutimana et al., 2023). Rice panicle architecture-related QTLs have also been reported elsewhere (Bai et al., 2021a). In this study we aim to dissect the panicle architecture of rice in terms of branching and lengths using a GWAS mapping population consisting of 158 rice genotypes. We identify QTLs for 20 traits (Table 1) using GWAS (Fig. 2). A comparative study of the expression of candidate genes between panicle and stem tissues was conducted using data obtained from the Rice RNA-seq database. A protein-protein interaction (PPI) analysis was performed using transcripts showing significant expression differences in the RNA-seq data analysis. A haplotype analysis was also conducted to identify novel candidate SNPs inherited together in a diverse array of rice genotypes. Additionally, epistatic interactions were assessed between SNPs with significant effects on rice panicles. Our findings provide the basis for detailed molecular analyses of panicle architecture traits in rice.

2. Material and methods

2.1. Plant materials and growing conditions

A collection of 282 accessions of rice were obtained from the International Rice Research Institute (IRRI, Philippines). Accessions were grown in an experimental field in a randomized complete block design with three replicates at Ahwaz (31°50'N, 48°27'E), Iran in 2021 and 2022. A total of 158 rice accessions (Table S1) reached panicle maturity. The accessions contained a mixture of landraces, breeding lines, varieties, and cultivars. Accessions belonged to TEJ (temperate japonica), IND (indica), AUS (aus), ARO (aromatic), TRJ (tropical japonica), and ADMIX subpopulations. Panicle traits were measured at maturity only from the main tiller, *i.e.*, the tallest panicle. Standard field management

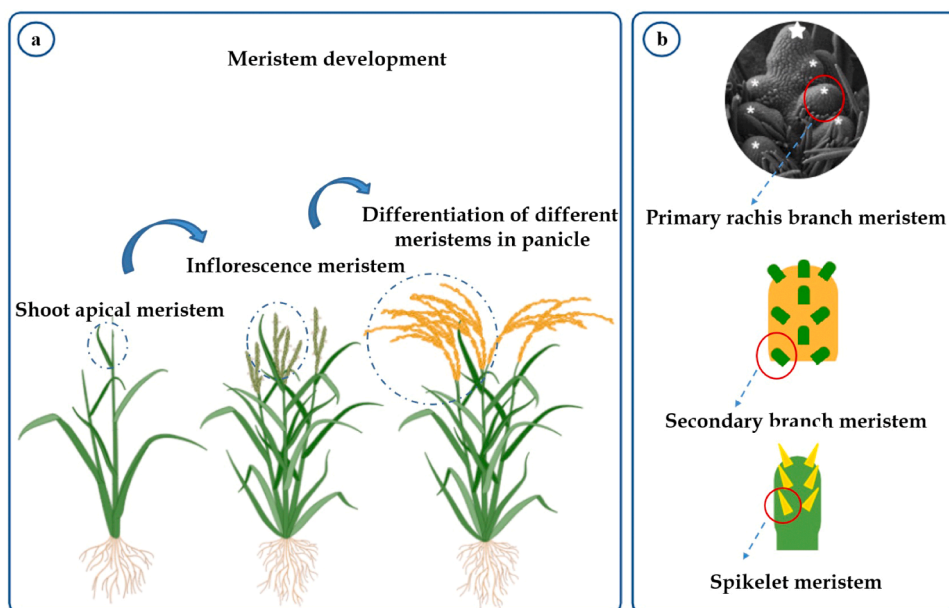


Fig. 1. Inflorescence meristem development stages in rice; a) rice panicle from the shoot apical meristem to inflorescence meristem. b) a scanning electron micrograph of the primary rachis branch meristem and a schematic representation of the primary and secondary rachis branch meristems and the spikelet meristem.

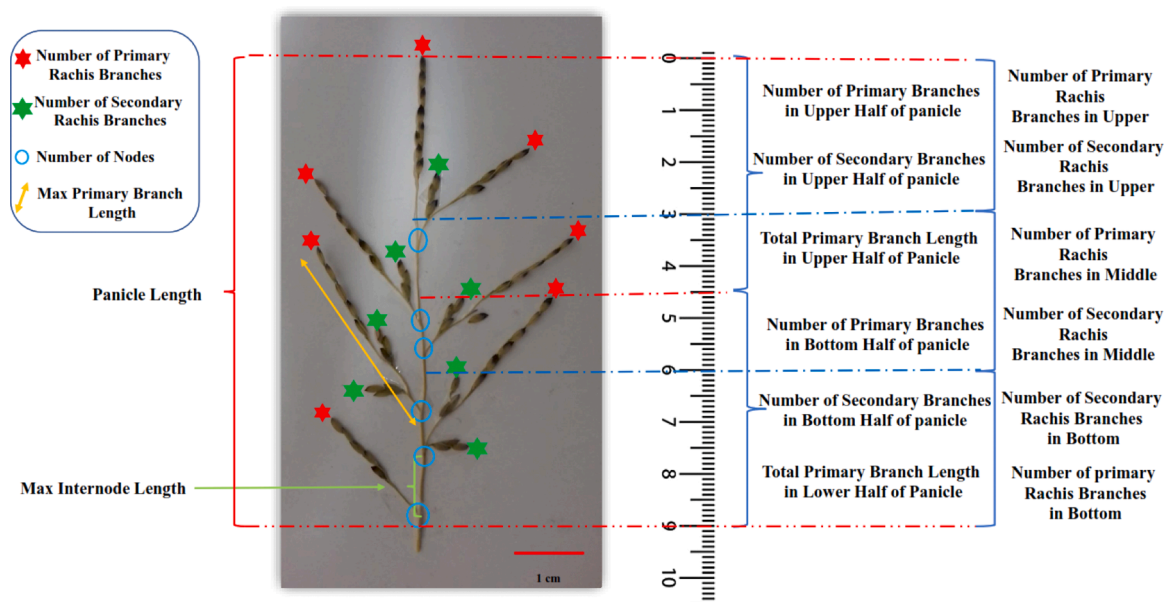


Fig. 2. Traits of rice panicle architecture: All panicles were fixed on paper near the ruler and the initial images were taken using a fixed camera (at the same distance from all panicles). In all images, the upper, the middle and the lower third of the panicle, and the upper and the lower halves of the panicle were identified. The images were analyzed in P-TRAP software (<https://www.quantitative-plant.org/software/p-trap>).

practices were performed throughout the growing season. Analysis of variance and mean comparisons (Duncan's multiple range test) were performed for all traits using the Agricolae packages in R.

Panicle traits were recorded by P-TRAP (Panicle TRAI Phenotyping; (Al-Tam et al., 2013)) for reliable and high-throughput accurate measurements of rice inflorescence architecture. The input was an RGB image of the spread panicle, fixed at the center on a white background. Adhesive tapes were used to stick the panicle onto the shooting stand. A total of 20 traits were analyzed in the current study and the traits and their description are listed in Table 1. The traits were obtained from reviewing the sources of all similar articles that have been published to date and from the USDA website (<https://www.ars.usda.gov/southeast-area/stuttgart-ar/dale-bumpers-national-rice-research-center/docs/rice-diversity-panel-1-rdp1/>). Considering that higher spikelet density at the top of the rice panicle is a selected trait, we examined all the traits that show this feature in the panicle. All data were entered in Excel following measurements and were used as phenotypic data for GWAS analysis performed in the R software (Fig. 2). Broad-sense heritability (H_b^2) for each trait was calculated based on the three replicates using the heritability package in R. The repeatability of these traits was measured using the Gaussian model implemented in the rptR package in R (<https://cran.r-project.org/web/packages/rpart/index.html>).

2.2. Linkage disequilibrium & genome-wide association studies (GWAS)

SNP genotyping using array hybridization has previously been described for rice by Zhao et al (Zhao et al., 2011). Single nucleotide polymorphisms (SNPs) information for all studied genotypes were downloaded from the Gramene portal (<http://gramene.org>). Briefly, 44, 100 SNPs from two data sources, the *Oryza* SNP project and the OMAP project were used for GWAS. Alleles were included in the final data if their minor allele frequency exceeded 0.05.

PCA was used for population structure analysis using the rMVP package (<https://cran.r-project.org/web/packages/rMVP/index.html>). GWAS analysis was performed using mixed linear models (MLM) (Zhang et al., 2010), the fixed and random model circulating probability unification (FarmCPU) model, and the general linear model (GLM) in rMVP. Fixed and FarmCPU analyses were performed using the first three principal components (PCs) (Liu et al., 2016; Panahabadi et al., 2021a)

to correct for population structure in the data set. Manhattan plots were generated using $-\log_{10}(p)$ values with the MVP package in R (Panahabadi et al., 2021a). SNP markers with $-\log_{10}(p\text{-value}) > 3.7$ were considered as significant SNPs, based on the quantile-quantile (Q-Q) plot. A phylogenetic tree and heatmap of kinship (K) matrix were created from the numeric SNP data using the Popkin package in R (Panahabadi et al., 2021b). Linkage disequilibrium analyses were performed using all 158 accessions in the association panel. The resolution of LDs was evaluated by pairwise calculations of LDs between 34,072 SNP markers. The value of r^2 in a sliding window of 50 markers was calculated using TASSEL and plotted graphically using ggplot2 in R to depicted LD decay with physical distance between SNPs (Luo et al., 2019).

2.3. Candidate gene identification

Based on the LD decay distance of each chromosome, we used regions extending half the LD decay distance flanking significant SNPs to identify putative candidate genes (Xie et al., 2021). To ascertain whether the candidate genes surrounding a QTLs have already been functionally characterized and to establish their relevance for panicle architecture, a thorough literature survey was carried out. Flanking genes with pleiotropic effects between traits were further examined

2.4. Gene expression analysis

The average gene expression for the GWAS candidate genes was calculated using RNA-seq data obtained from two neighboring tissues, panicle and stem. The expression data for panicle (young panicle-milky stage; R6 flowering stage) representing reproductive tissues and stem (three-leaf stage), representing vegetative tissues, was obtained from the Rice RNA-seq Database (<http://ipf.sustech.edu.cn/pub/ricerna/>), to identify genes possibly involved in panicle formation. The quantitative analyses were conducted based on read counts using FPKM values (expected number of fragments per kb per million reads) for each candidate gene. Samples with many zeros were removed. Read counts were normalized on a per sample basis using a normalization factor obtained from the sum of each sample divided by the sum of the smallest sample. To identify differentially expressed genes (DEGs), the R packages limma, edgeR, and umap were used with the threshold of "adjusted p -values" set

Table 1

List of trait names, abbreviations (symbol), descriptions, and units that were measured in this study. The traits are depicted in Fig. 2.

Trait name	Symbol	Trait description	Measurement Unit
Panicle Length	PL	length of a panicle from the base to the tip	cm
Number of Nodes	NN	total number of nodes rachis	number/panicle
Total Number of Primary Rachis Branches	NPRB	total number of nodes on the panicle axis from base to tip	number/panicle
Total Number of Secondary Rachis Branches	NSRB	total number of secondary branches on the panicle from base to tip	number/panicle
Number of Primary Rachis Branches in Upper	NPRBU	number of primary rachis branches in the upper third of the panicle	number
Number of Primary Rachis Branches in Middle	NPRBM	number of primary rachis branches in the middle third of a panicle	number
Number of Primary Rachis Branches in Bottom	NPRBB	number of primary rachis branches in the lower third of a panicle	number
Number of Secondary Rachis Branches in Middle	NSRBM	number of secondary rachis branches in the middle third of a panicle	number
Number of Secondary Rachis Branches in Bottom	NSRBB	number of secondary rachis branches in the lower third of a panicle	number
Number of Primary Branches in Upper Half of Panicle	NPBUH	number of primary branches in the top half of a panicle	number
Number of Primary Branches in Bottom Half of Panicle	NPBBH	number of primary branches in the bottom half of a panicle	number
Number of Secondary Branches in the Upper Half of Panicle	NSBUH	number of secondary branches in the top half of a panicle	number
Number of Secondary Branches in the Bottom Half of the Panicle	NSBBH	number of secondary branches in the bottom half of a panicle	number
Number of Internode	NI	distances between two nodes	number
Max Internode Length	MIL	the greatest distance between two nodes on the rachis	cm
Total Primary Branch Length	TPBL	total length of primary branches in panicle	cm
Total Primary Branch Length in Upper Half of Panicle	TPBLUH	total length of primary branches in the upper half of a panicle	cm
Total Primary Branch Length in Lower Half of Panicle	TPBL LH	total length of primary branches in the lower half of a panicle	cm
Max Primary Branch Length	MPBL	length of the longest primary branch among the branches of a panicle	cm
Total Number of Spikelets in Panicle	TNSP	total number of spikelets in a panicle from the base to the tip	Number/panicle

Secondary branch meristems are being produced successively on the primary branch to differentiate into spikelet branch meristems and lateral spikelet meristems. Concurrently, the top of the primary branch meristem differentiates into a terminal spikelet meristem (Fig. 1b) (Li et al., 2020). Each primary branch meristem generates next-order meristems laterally until they acquire inflorescence meristem identity. Floral organs develop from the flanks of the floral meristems to make grains (Zhuang et al., 2020).

to less than 0.05 and $|\log_2 \text{Fold change}| > 1$. A volcano plot was drawn using the tidyverse and ggrepel packages, showing up- or down-regulated genes together with all non-significant genes. A heatmap was generated from the RNA-seq data of the candidate genes displaying substantial differences in gene expression between the two tissues with gplots R package. To get an overview of different functional classes present in the DEGs, a Gene Ontology (Go) analysis was performed using PANTHER (<https://www.pantherdb.org/geneListAnalysis.do>) with an ID list containing all significant DEGs. A protein-protein interaction network was established between DEGs using STRING (<https://string-db.org/>) using a minimum required interaction score: medium confidence of 0.4) in Cytoscape (V, 3.10.2, algorithm, BottleNeck). Hub genes were colored yellow, and a protein-protein interaction network between genes with $\log_2 \text{FC} > 3$, for a total of 31 genes, was drawn in STRING.

2.5. Haplotype and epistatic analysis

For the haplotype analysis, phenotypic, genotypic, cultivar, and bed files including the positions of genes in the identified QTLs were used. Haplogroups consisting of less than five accessions were excluded. Haplotype analysis was performed for SNPs within 500 kbp intervals. GeneHapR, an R package, was used to perform haplotype analyses for all gene blocks of each trait and the corresponding images were generated. To determine potential epistatic interactions between different QTLs influencing inflorescence architecture, we performed an epistatic interaction analysis using functional regression with FRGEpistasis (Weng et al., 2014).

3. Results

3.1. Population structure and LD decay

The phenotypic distributions for all traits are shown in Figure S1. The mapping population consisted of accessions from six different sub-populations according to Zhao et al (Zhao et al., 2011). (ADMIX, AROMATIC, AUS, IND, TEJ, TRJ). The phenotypic variation of the measured traits is summarized in Table S2. The principal component analysis (Figure S2) identified four subgroups. At the same time, the kinship matrix, a summary of the distribution of pairwise relative relationship coefficients among accessions, could be grouped into five sub-populations of temperate japonica, indica, Aus, aromatic, and tropical japonica (Figure S3). LD decays for all chromosomes are presented in Figure S4. The distance where LD drops by 50 % varied from 200.1 to 700.2 kbp across the different rice chromosomes (Table S3). The distribution of SNP markers on each chromosome is provided in Figure S5, which shows the highest and the lowest SNP abundances are found on chromosomes 1 and 10, respectively. On average, a SNP was observed every 10,955 bp across the rice genome (Table S3).

3.2. GWAS results

In this study, 34,072 SNPs were used for GWAS analyses. Based on the Manhattan plots (Fig. 3 and S6), 52 SNPs, with $-\log_{10}(p)$ value ≥ 3.7 , were found to be associated with a total of 19 traits. Significant SNPs were distributed on all chromosomes (Table S4). Traits sharing associated SNPs are listed in Table S5. The peak markers, $-\log_{10}(p)$, candidate genes, QTLs, candidate gene IDs are presented in Tables S6 and S7 while gene functions associated with candidate genes are presented in Tables S8. Based on a comparative analysis of Q-Q plots comparing the three GWAS models we used (MLM, GLM, and FarmCPU), we chose to present the results from FarmCPU since it displayed the most marker-trait associations ($-\log_{10}(p) > 3.7$) for all traits (Fig. 3 and S6). The repeatability and heritability of traits are reported in Table S9.

Pleiotropy occurs when one gene affects more than one trait and contributes to the genetic correlation between traits (Auge et al., 2019). Pleiotropy with linkage disequilibrium results in genetic correlations

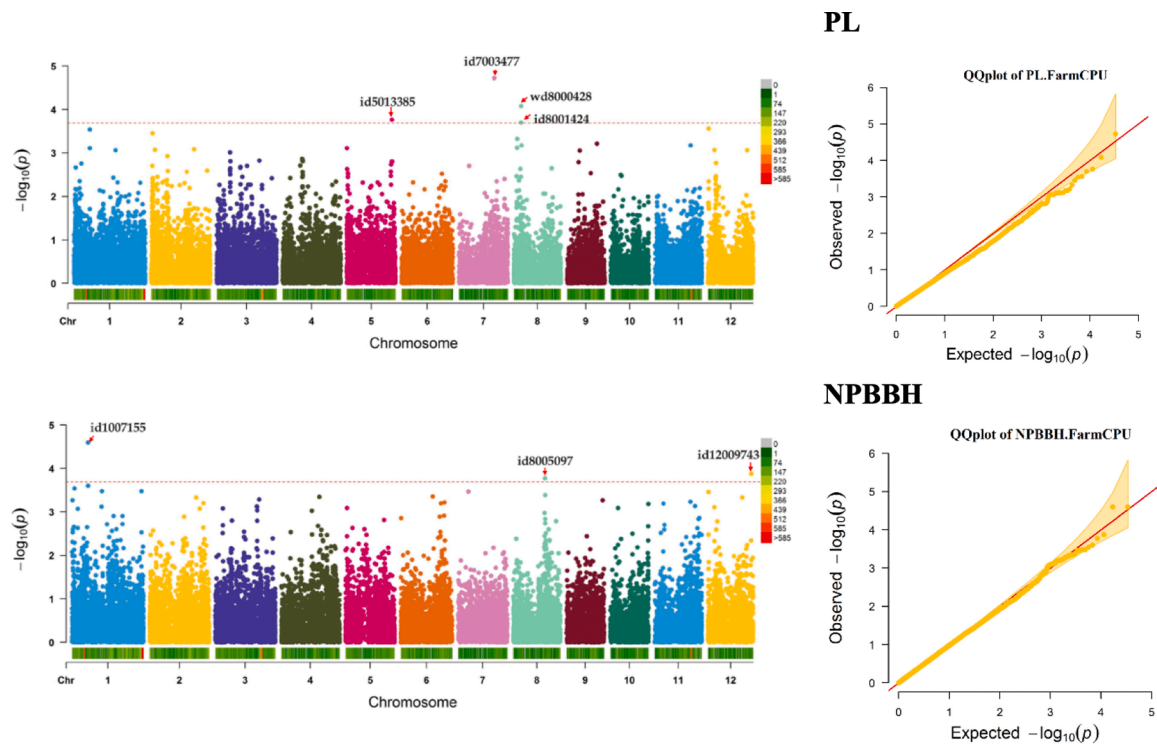


Fig. 3. Manhattan plots (two traits, *i.e.*, PL and NPBBH, are shown, please see the [Supplementary Figures](#) for the other traits) showing marker-trait associations in genome-wide association study results using the FarmCPU model. The blue line on each Manhattan plot indicates significant marker-trait associations with $-\log_{10}(p) > 4$. The quantile-quantile plot (on the right) illustrates the distribution of expected vs. observed probability values, represented based on $-\log_{10}(p)$.

between traits due to physical linkage or population structure (Chebib and Guillaume, 2021). Genes with pleiotropic effects with potential functions on several traits are reported in [Table S10](#). The pleiotropic genes include *peptidase*, *protein kinase*, *ubiquitin*, *Kelch*, *Zinc finger*, *Cytochrome P450*, *pentatricopeptide*, *DUFs*, *tetratricopeptide*, *WD40* and *MYB transcription factors*.

3.3. Differentially expressed candidate genes between stem and panicle

A heatmap for all candidate genes was generated from the gene expression data (FPKM values are reported in [Table S11](#)). Genes that show significant differences in gene expression values between two neighboring tissues, panicle and stem, are displayed in [Figure S7](#). The purpose of comparing the expression of candidate genes between panicle and stem tissues was to shortlist and identify genes with substantial roles in panicle formation. We identified a total of 211 DEGs, 103 of which were up-regulated and 108 of which were down-regulated ([Figure S8](#)), \log_2FCs reported in [Table S12](#). A PCA was performed on all RNA-seq data related to the candidate genes identified from the GWAS study. The data before and after normalization are shown in [Figure S9](#). Gene expression comparisons of the normalized data were performed between the two tissues.

Heatmaps of genes with up- and down-regulation in the panicle compared to the stem are shown in [Figure S7](#) and [Figure S10](#). Amongst those with high fold change ($\log_2FC \geq +3$) in the panicle and down-regulated genes ($\log_2FC \leq -3$) in the panicle reported in [Table S13](#).

The functional annotation of GO terms was performed based on the molecular function (MF), biological process (BP), cellular component (CC), and protein class (PC) to identify the biological meaning and the systematic features of 211 DEGs. [Figure S11A](#) summarizes the eight molecular functions to which all the activities belong: 75.7 % of the data consisted of unclassified genes while the rest belonged to catalytic activity (Go: 000003824, 17.5 %), binding (GO: 0005488, 7.8 %), transcription regulator activity (GO: 0140110, 2.9 %), transporter activity

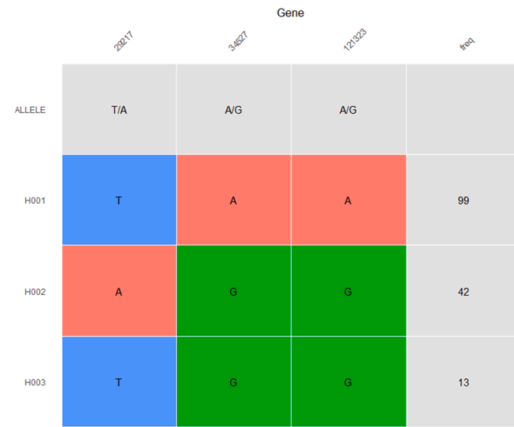
(GO: 0005215, 1 %), ATP-dependent activity (GO: 0140657, 1 %), cytoskeletal motor activity (GO: 0003774, 0.5 %), and molecular function regulator activity (GO: 0098772, 0.5 %). The overrepresented GO terms for the biological processes contained more than half of the data, including 18.9 % metabolic process (GO: 0008152), 16 % cellular process (GO: 0009987), 7.8 % biological regulation (GO: 0065007), 6.8 % response to stimulus (GO: 00500896), 1.9 % biological process involved in interspecies interaction between organisms (GO: 0044419), 1.5 % developmental process (GO: 0032502), 1 % localization (GO:0051179), and 0.5 % homeostatic process (GO: 0042592) with the rest as unclassified ([Figure S11B](#)). The cellular component in which these targets perform their function was categorized as 75.7 % unclassified ([Figure S11C](#)). The rest belong to the cellular anatomical entity (GO: 0110165, 23.3 %) and protein-containing complex (GO: 0032991, 2.4 %). For protein class terms ([Figure S11D](#)) 59.2 % were grouped as unclassified. Transmembrane signal receptor (PC00197) and protein modifying enzyme (PC00260) were 10.2 % of each, while metabolite interconversion enzyme (PC00262, 7.3 %), gene-specific transcriptional regulator (PC00264, 5.3 %), defense/immunity protein (PC00090, 1.9 %), scaffold/adaptor protein (PC00226, 1.5 %), cytoskeletal protein (PC00085, 1 %), protein binding activity modulator (PC00095, 1 %), RNA metabolism protein (PC00031, 0.5 %), transporter (PC00227, 1 %), and DNA metabolism protein (PC00009, 0.5 %) were accounted for less than 10 % of classes each.

3.4. Protein-protein interaction analysis

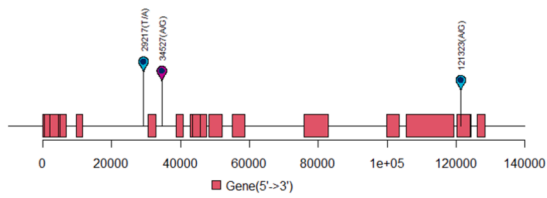
The results of the PPI network analysis of all DEGs ([Figure S12a](#)) and DEGs that had a $|\log_2 FC| < 3$ are shown in [Figure S12b](#). All accessions in the PPI network are shown in [Figure S12](#). We added 31 genes with $|\log_2 FC| > 3$ to the STRING database. Hub genes are shown yellow in [Figure S13](#). Accessions that did not interact were removed and 13 genes were kept that interacted with each other ([Figure S12b](#)). The hub gene accessions and functions are reported in [Table S14](#).



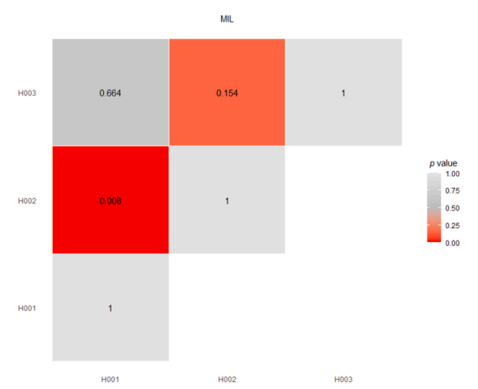
a



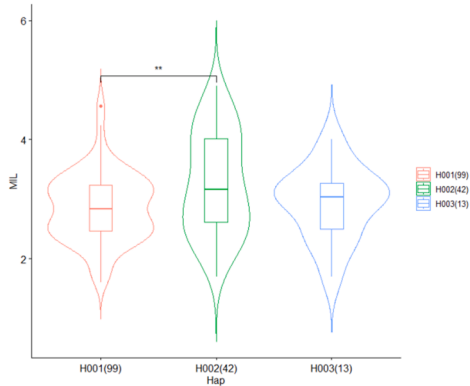
b



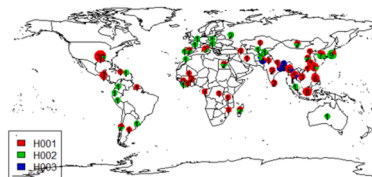
c



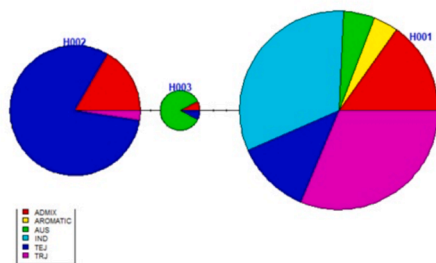
d



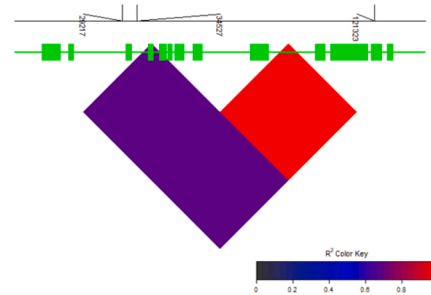
e



f



g



h

(caption on next page)

Fig. 4. Haplotype analysis in qMIL2 region for MIL (Max Internode Length) located on Chromosome 2. a) at first six haplogroups were observed in 158 accessions using three SNPs: colored boxes are illustrative of haplotype variants with the corresponding frequency at the last column. * significant at $p \leq 0.01$. b) three haplogroups had more than five accessions and other groups were removed. c) gene models associated with qMIL2: visualization of variants position above gene model, the black line represents the genome and rectangles represent upstream and downstream variants. d) heatmap for phenotypic differences in haplogroups. e) violin plot shows the comparison of MIL among accessions between the three haplotypes of qMIL2 (f) geo-distribution of major haplotypes of qMIL2; circle size represents accessions counts and the pies in different color represent constituent ratios of classified haplotype categories for relevant accessions derived from different eco-regions. H003 is found only in Asia, while H001 and H002 are found globally. (g) qMIL2 haplotype network. Each circle represents a haplotype and the size indicates the accession number. The pies in different colors represent the ratio of category in each haplotype. The symbol on the line between haplotypes represents the number of variants. (h) LD-block visualization of each site in the locus. LD-block and its red color indicate the close relationship between the SNPs of this haplotype block. The gene model was presented at the top of the plot, the line represents the genome and the rectangle represents the upstream gene variant and downstream gene variant. The LD block with the color key lies at the bottom.

3.5. Haplotype and epistatic analysis

Haplotype analysis for all significant SNPs resulted in seven chromosomal blocks for four traits (NSRBB, NSBBH, MIL, and NPBUH) that harbored at least three significant SNPs. Amongst them, the SNPs for MIL and NSBBH were located in coding regions (Fig. 4 and S14). The haplotype analysis of MIL (Max Internode Length) identified three haplotypes of qMIL2 in the population located on chromosome 2 (Fig. 4, b). These three haplotypes included haplotypes H001 (present in 99 accessions), H002 (present in 42 accessions) and H003 (present in 13 accessions). The phenotypic value for H003 was not significantly different from the other two haplotypes (H001 & H002). However, individuals carrying haplotype H002 displayed larger MIL values than individuals with haplotype H001 (Fig. 4). The violin plot of qMIL2 for the three haplogroups showed a significant difference between the two haplotypes. According to geo-distribution, H003 belongs to the accessions that originated from Asia, while H001 and H002 were found everywhere. H001 includes more accessions from the TRJ and IND groups while individuals in TEJ were mostly found to carry H002 or H003, including AUS (Fig. 4). In these haplogroups, SNPs resided in the gene of *inositol monophosphatase family protein*: id2002053 [POS: 3793906 with missense conversion (A→G) resulting in Trp to Cys] and id2001992 [Pos: 3707110 with a transition (A→G) upstream of the ORF]. Here, the population was divided into three significant haplotypes for MIL, H001 found in 99 accessions with a mean of 2.86, containing TRJ, IND, and TEJ individuals, H002 found in 42 accessions with mean of 3.23, mainly consisting of individuals from TEJ, and H003 found in 13 AUS accessions with a mean of 2.94. The significant difference seen between the H001 and H002 haplotypes is probably due to the presence of IND accessions, cultivars that display longer and larger panicles (the number of primary and secondary branches, and the length of the panicle is greater) than japonica accessions (Bai et al., 2021b) in H001.

Haplotype analysis of NSBBH (Number of Secondary Branches in Bottom Half of panicle) resulted in four haplogroups. qNSBBH21 region on chromosome 2 within 158 accessions was a haplogroup based on the presence of five significant SNPs. A violin plot of qNSBBH21 for the four haplogroups demonstrated no significant differences between the four haplotypes. Haplotype H001 is found mostly in Asia, while H002, H003 are found everywhere, and H004 are found in Asia and Africa. H001 includes more IND individuals, H002 includes more individuals from TEJ, H003 includes more individuals from TRJ while H004 includes more individuals from the Aromatic group. (Figure S14). The id2007248 SNP is a T→C transition located downstream of the ORF.

We identified epistasis between chromosomes 1 (SNP2 that includes *myosin heavy chain-like protein*, *Dof*, *DUF688*, *permease*, *dynein light chain*, *homeodomain*, *DUF2039*, *TCP family transcription factor strigolactone* and *cytokinin controlled mesocotyl elongation in darkness*, *cytochrome P450*, *DUF155*, *pentatricopeptide repeat*, *Zinc finger*, *RING finger*) and 9 (SNP1 that includes *DUF573*, *DUF1644*, *peptidase A1*, *ubiquitin*, *peptidase S26A signal peptidase I*, *peptidase S9A prolyl oligopeptidase*, *peptidase S54 rhomboid*, *heat shock*, *remorin*, *BZIP transcription factor*, *cytochrome P450*, *AP2*, *DUF827*, *brassinosteroid signaling control of organ length*) for a number of NSRBB traits (Table S15).

4. Discussion

Rice yield is highly dependent on panicle architecture. therefore, it is important to identify the genes that are involved in determining panicle architecture for use in selection programs, to design smart crossing blocks, and to define the ultimate ideotype. We used a GWAS approach to assess how genotypic diversity available in a diverse array of 158 rice accessions, collected from across the world, help control the structure and morphology of the rice panicle. Three GWAS models, *i.e.*, FarmCPU, GLM, and MLM models were tested and FarmCPU was ultimately selected for identifying SNPs significant associated with our traits of interest that would serve as proxies for candidates involved in defining each of the 20 panicle traits we included in our study. According to earlier studies, the statistical power of FarmCPU is greater than the other GWAS models (Zhong et al., 2021). The pattern of LD decay is influenced by the genetic structure of the population, *i.e.*, the population size and composition, the density of SNP markers, the number of SNPs and the distribution of SNPs across chromosomes (Hao et al., 2022). All panicle-related traits had high heritabilities, in line with earlier studies (Adam et al., 2023; Chen et al., 2023). We identified 52 significant SNPs, (Lu et al., 2015) QTLs, and a total of 876 protein-coding genes as candidates for all traits included in our study (Table S7).

Previously, and similar to our findings, the roles of genes such as *Kelch* (Zhang et al., 2012a), *remorin* (Gui et al., 2014), *patatin-related phospholipase* (Liu et al., 2015), *Dof* (Deveshwar et al., 2020), *AP2* (Li et al., 2021a), and *NB-ARC* (Sinha et al., 2023) have been implicated in defining panicle architecture. *OsDof12* is related to rice architecture by influencing plant height, NPRB, NSRB, number of spikelets per panicle, and overall panicle size (Ta et al., 2018). *OsDof12* appears to regulate panicle architecture via a negative regulatory feedback loop of BR signaling (Deveshwar et al., 2020). *OsDof12* also reduces NSRB (Wu et al., 2015). We identified several *Dof* members in the flanking region of association signals for traits such as NPRB, NPBBH, and NSRBB. The *AP2/ERF* family of TFs affects NPRB, NSRB, and rice panicle architecture (Harrop et al., 2019), controlling panicle morphology traits (Luong, 2019). In our study, *AP2* paralogs were shown to be associated with NSRB, NSRBB, NPRBU, and NSBBH. An earlier GWAS indicated the role of *GNP12*, an NB-ARC, as a positive regulator of panicle growth and length (Rashid et al., 2023). However, the mechanism of action has not yet been established. It has also been shown that rice NB-ARC probably improves PL (Sinha et al., 2023). Here, NB-ARC family members were associated with PL, NPRBM, NPBUH, NPBBH, NI, MPBL, and TPBLH (Table S7). Structural proteins, such as remorins, may play a definitive role in the overall structure of a cell, tissue, or organ. Remorins are plant-specific and plasma membrane-associated proteins that play an essential role in plant growth and development (Narawatthana et al., 2023) via stabilizing large-scale membrane conformations independent of the cell wall (Su et al., 2023). Remorin is related to internode length and PL (Gui et al., 2014). In our study, *remorin* homologs were associated with PL, NSRBB, NPBUH, NPRBU, and TPBLH traits. Patatin-related phospholipase A (*pPLA*), a glycerolipid hydrolase, has been shown to play a role in rice vegetative and reproductive growth as a suppressor of cell elongation probably leading to shortened panicles (Liang et al., 2014; Zhang et al., 2021). In our study *Patatin* was observed flanking an

Table 2
List of previously reported candidate genes with $\log_2FC > 3$.

Gene name	Reported Trait names	Reference	Trait name
<i>RING-like Zinc-finger</i>	rice panicle branching architecture- morphology plant growth and development flower development	(Wang et al. 2008; Zheng et al. 2022). (Xiao et al. 2009)	NPRB, NSRB, NN, PL, NSRBB, NPRBU, NPRBB, NPBBH, NSBBH, NI, MIL, and TNSP
<i>bHLH</i>	grain size by influencing cell numbers - longitudinal direction of spikelet hulls cell division number of secondary branches in the panicle number of primary panicle and secondary panicle branches	(Yang et al., 2018) (Luo et al. 2013) (Seo et al. 2020) (Lv et al. 2023)	PL, NSRB, NSRBB, NPRBU, NPBUH, NSBBH, and MPBL
<i>Kelch repeat gene</i>	rice heading-date genes heading date floral activators in sorghum flowering independent of photoperiod dependent promotion of flowering plant architecture regulation floral organ number and size floral morphology cell division grain length	(Zhang et al. 2022) (Tadesse et al. 2024) (Han et al. 2015) (Imaizumi et al. 2005). (Li et al. 2011) (Zhang et al. 2012; Hu et al. 2012)	NSRB, NN, PL, NPBBH, NSBBH, NI, MIL, MPBL, and TPBLLH.
<i>Peptidase</i>	regulate rice architecture by influencing polar auxin transport tiller and panicle numbers	(Zhao et al. 2015) (Wu et al. 2023)	NPRB, PL, NSRBB, NPRBU, NPBUH, NPBBH, NSBBH, NI, MIL, TPBL, MPBL, TPBLUH, TPBLLH, and TPBLLH
<i>cytochrome P450</i>	differentiation of spikelet primordial, panicle branches inflorescence architecture in rice negative role in gibberellin-mediated regulation of cell elongation in the uppermost internode of rice plant height, rice panicle development, main rachis growth improved grain per panicle and seed setting rate in rice inflorescence architecture in rice plant growth regulation that affects plant height grain number and size increase in grain size, weight, and yield in rice	(Luo et al. 2006). (Guo et al. 2014) (Qian et al. 2017) (Li et al. 2018) (Zhao et al. 2022) (Zhou et al. 2017) (Fang et al. 2016; Zhou et al. 2017; Aloryi et al. 2022)	NSRB, NSRBB, PL, NPRBB, NPBUH, NSRBB, NPBUH, NSBBH, MIL, NI, MPBL, and TNSP.
<i>Protein ubiquitination</i>	stem cell processes in young rice panicles panicle size and the grain number in rice regulation of grain width and size in rice	(Zhu et al. 2020) (Huang et al. 2021) (Shi et al. 2019)	NPRB, NSRB, NSRBB, NPRBU, NPBUH, NPBBH, NSBBH, MIL, MPBL, TPBLUH, TPBLLH, and TNSP
<i>Protein kinase</i>	regulating the process of plant architecture establishment grain size in rice-cell proliferation regulates rice panicle architecture increased plant height and primary branches per panicle grain size, panicle size, primary branches, and secondary branches panicle morphogenesis panicle architecture denser panicles	(Wu et al. 2018) (Duan et al. 2014) (Guo et al. 2023) (Zou et al. 2015) (Xu et al. 2020) (Guo et al. 2018)	NN, PL, NSRBM, NSRBB, NPRBU, NPRBM, NPBUH, NPBBH, NPBBH, NSBBH, NI, MIL, TPBL, MPBL, TPBLUH and TPBLLH

SNP associated with TPBLLH. The list of all genes in discussion for all traits is reported in Table S16.

After examining the DEGs between stem and panicle, and performing functional annotation via GO, it was determined that predictions based on molecular function were not informative. Interestingly, GO terms for biological processes of DEGs were informative as they explained the roles of DEGs in metabolic and cellular processes, biological regulation, and developmental processes; all were within the scope of panicle development and architecture. The cellular component and protein class terms were not informative as the majority of the terms were unclassified. This means that enhancements to the GO software are likely required. We therefore performed a transcriptome data analysis between stem and panicle tissues. The differentially expressed genes between the two tissues included genes that had previously been reported to be involved in panicle definition, and this then serves that the method works. These analyses also allowed us to shortlist novel genes that have previously not been linked to panicle formation.

4.1. Candidate genes with significant transcript expressions

To confirm the results from our GWAS analyses and to identify candidate genes involved in rice panicle formation, we performed the

gene expression analysis between two tissues (panicle and stem). Our analysis highlighted some genes with increased panicle expression ($\log_2FC > 3$, Table 2). From this list, some genes have already been reported as being involved in the definition of the panicle architecture, including *RING-like Zinc-finger protein* (Wang et al., 2008; Zheng et al., 2022), *C2H2 zinc finger* (Xiao et al., 2009), *bHLH* (Luo et al., 2013; Yang et al., 2018; Seo et al., 2020; Lv et al., 2023), *Kelch repeat gene* (Li et al., 2011; Zhang et al., 2012b; Hu et al., 2012), *Peptidase* (Zhao et al., 2015; Duan et al., 2019b), *Cytochrome P450* (Luo et al., 2006; Guo et al., 2014; Zhou et al., 2017; Aloryi et al., 2022; Sahoo et al., 2023), *Protein ubiquitination* (Shi et al., 2019; Zhu et al., 2020; Huang et al., 2021) and *Protein kinase* (Duan et al., 2014; Zou et al., 2015; Guo et al., 2023). Furthermore, Table 3 lists genes with reduced panicle expression ($\log_2FC < -3$), including *Pentatricopeptide repeat* (Jiang et al., 2014; Ke et al., 2018), *Tetratricopeptide (TTP) proteins* (Harrop et al., 2019; Khong et al., 2021), *Rice WD40s* (Kwon et al., 2012; Yoshida et al., 2012; Yang et al., 2021), *Homeodomain* (Bai et al., 2021a; Li et al., 2021b), *RING Finger Protein ligase* (Yan et al., 2022), *TCP family transcription factor* (Nakagawa et al., 2012; Zhang et al., 2014; Ming et al., 2023) which have previously been reported as involved in panicle architecture.

Table 3
List of previously reported candidate genes with $\log_2FC < -3$.

Gene name	Trait reported in other articles	Reference	Our traits
Pentatricopeptide repeat	regulating peduncle and secondary branch elongation differences in branch numbers and spikelet per panicle	(Jiang et al. 2014)	NSRB, NN, PL, NSRBB, NPRBU, NPRBB, NPBUH, NPBBH, NSBBH, NI, MIL, TPBL, MPBL, TPBLUH and TPBLH
		(Ke et al. 2018)	
Tetratricopeptide (TTP) proteins	control the number of spikelets by controlling primary and secondary branches in rice panicles controlling the number of spikelets the number of secondary branches	(Harrop et al. 2019)	NSRB, NSRBB, NPRBU, NPRBB, NPBUH, NSBBH, NI, PL, NSRBB, NPRBU and NSBBH
		(Khong et al. 2021)	
Rice WD40s	panicle branch number regulate grain number through the control of secondary branches axillary meristem inflorescence development controls increased kernel row number seed size and the number of lateral branches	(Ojolo et al. 2018)	NSRB, NN, PL, NSRBM, NSRBB, NPRBU, NPRBM, NPBUH, NPBBH, NSBBH, NI, TPBL, MPBL, TPBLH, and MIL
		(Chen et al. 2021)	
		(Kwon et al., 2012; Yoshida et al., 2012)	
		(Yang et al. 2018a)	
Homeodomain	regulating normal panicle architecture clustered primary branches and short rachis	(Bai et al. 2021; Li et al. 2021)	NSRB, PL, NSRBB, NPRBU, NPBUH, NSBBH, NSBBH, TPBLUH, and TPBLH
RING Finger Protein ligase	regulates flowering time, the number of grains in the panicle, the number of primary branches, the number of tillers, and the plant height regulates the rice panicle seed setting rate	(Yan et al. 2022)	NSRBB
TCP family transcription factor	tillering and branching in rice and Arabidopsis elongation of organs and the internodes of rachis branches through decreased cellular proliferation controls branching in Arabidopsis	(Zhang et al. 2014)	NSRBB
		(Nakagawa et al. 2012; Zhang et al. 2014)	
		(Xie et al. 2020)	

4.2. Novel candidate genes

The genes that have not previously been reported for the traits of study or to be associated with panicle architecture were considered novel genes. For example, *Ankyrin* genes have been reported to control rice panicle architecture and secondary branch diversity in panicle (Khong et al., 2021). *Ankyrin* homologs were identified in the flanking regions of SNPs associated with NN, NI, NSRBB, NPBBH, TPBL, MPBL, and NPBUH. Similarly, *Duf* homologs have been shown to have roles in the development (Nabi et al., 2020) and to control the shape and size of rice grain, likely by altering cell division and expansion of the grain hull (Yan et al., 2013). Paralogs of this gene were observed in the flanking regions of SNPs associated with NN, NI, PL, TNSP, MIL, TPBL, MPBL, TPBLH, TPBLUH, NSRB, NSBBH, NSRBM, NSRBB, NPRBU, NPRBM,

NPRBB, NPBUH, NPBBH.

Leucine-rich repeat receptor-like kinase (LRR-LRK) over-expression in rice led to increased panicle, spikelet in panicle, weight per grain, increased cellular proliferation, and the grain yield per plant (Zha et al., 2009). *Leucine-rich repeat* homologs were identified in the flanking regions of SNPs associated with NN, NI, NSRBB, NSBBH, NPBBH, NPBUH, NPRBU, MIL, and MPBL. *KIP1-like domain-containing proteins*, known as ICKs (inhibitors of cyclin-dependent kinase, CDK) or KRPs (Kip-related proteins), function to regulate the activities of CDK through cell cycle regulation (Ajadi et al., 2019). *KIP* homologs were observed in the flanking regions of SNPs associated with NN, NI, and NPRBU. The *Brassinosteroid insensitive 1-associated kinase 1-like* gene is strongly expressed in rice panicles, suggesting that this gene plays a role in grain growth and development (Teh et al., 2019). BRs levels in rice panicles promote spikelet development, enhance inflorescence meristem activity and panicle growth (Xie et al., 2019). We found homologous genes of BRs in the flanking regions of SNPs associated with NN, NI, and NSRBB.

Several *Kinesins* have been reported to be involved in plant development, many cellular functions and morphogenetic processes, cell division (Kitagawa et al., 2010), cell plate formation (Fang et al., 2018), cell elongation control, grain shape (Kitagawa et al., 2010), control of plant height, tillering (Ran et al., 2018), glume length (Fang et al., 2018), grain length (Wu et al., 2014), weight (Ye et al., 2022) and width through the cell proliferation (Ran et al., 2018). We found homologs of this gene in the flanking regions of SNPs associated with NPBBH and NPRBU.

R2R3 MYB TF has been reported to affect grain number, and panicle architecture, and to control flower and spikelet development (Li et al., 2022a, 2022b). *MYB TFs* were identified in the flanking regions of SNPs associated with NPRB, NN, NPBUH, NPBBH, and MPBL. Alos, *Glucanases*, among many other roles, are required for root cell elongation and cell division in rice, and internode cell elongation (Zhang et al., 2012a). We observed this gene in the flanking of an SNP associated with PL which has the possibility of influencing PL elongation.

Interestingly, some of the associated genes had pleiotropic effects on rice panicle architecture in our post-GWAS analysis such as *Pentatricopeptide*, *Tetratricopeptide*, *WD40*, *Homeodomain*, *DUFs*, *Brassinosteroid insensitive* and *MYB TF* (Table S10). It should be noted that several genes with pleiotropic effects on panicle traits have already been reported in previous studies. Pleiotropy occurs when a single mutation or gene/allele affects more than one phenotypic trait. Pleiotropy is an important concept in population genetics that explains why certain traits are always found together among individuals in a population (Christoffers, 2018; Zimdahl, 2024).

The development of the panicle system plays a vital role in increasing the yield of rice. This requires the identification of proteins that play a significant role in panicle formation and architecture. PPI network analysis is used to enhance our global understanding of important proteins governing panicle formation. Computational approaches in creating higher-level views of biological systems (such as PPI network graphs are useful for identifying complex relationships between proteins (Wimalagunasekara et al., 2023). Here, we identified 211 proteins that were observed to have significant transcript differences between panicle and stem. Of these, 52 proteins were included in our construction of a PPI network, and after reviewing the sources, it was determined that these proteins probably play a role in panicle formation. This network provides ways to identify important members of the central modules of panicle formation. Hub proteins (yellow circles, Figure S11) are potential candidates for future genetic engineering experiments because their impact on panicle formation is greater than other proteins. The role of some of these hub proteins, such as zinc finger (Wang et al., 2008; Zheng et al., 2022) and ubiquitin (Shi et al., 2019; Huang et al., 2021), in controlling panicle structure has already been experimentally confirmed. Others, such as Ankyrin, Dufs, and heat shock proteins, need further experimental verification before their contributions to panicle traits are fully understood.

4.3. Haplotype and epistasis

A haplotype is a collection of alleles, SNPs or other variation such as indels, that are inherited together and are physically located in the same region of a chromosome (Christoffers, 2018). Knowing haplogroups is useful in concurrent breeding for more than one trait. Therefore, developing markers that can differentiate haplotypes will help increase the breeding speed during selection years. For example, when we are looking for rice with longer panicle in our study, *i.e.*, MIL traits, it is better to choose parents carrying haplotype H002. Developing markers for NSBBH would help analyze the germplasms received from international collections to differentiate the genotypes into subgroups and use them more effectively in crossing schemes for the trait of interest, *i.e.*, NSBBH that can be considered as a yield-definitive trait. Although there were no significant differences between the four haplogroups in our study, the study and separation of the population based on these haplogroups can be used to identify panicles with more grains.

Studying epistasis between the two loci is a natural step following a single locus analysis. There are complex relationships between genes that have epistatic effects, for example, two of the brassinosteroid biosynthesis genes that encode *cytochrome P450s*, whose function is to influence the regulation of plant architecture (Sakamoto et al., 2006). Mutants with altered rice panicle morphologies, such as different secondary branches *PMM1* (Li et al., 2018), *GNS4* (Zhou et al., 2017), *CPB1* (Wu et al., 2016) and *NBG4* (Tong et al., 2018) all resulted from different alleles at *DWARF1* (encoding a cytochrome P450). The *DOF* transcription factor (*OsDof12*), plays a role in determining the number of secondary branches in the rice panicles and this gene is a negative regulator of brassinosteroid signaling (Wu et al., 2015). *OsDof12* may be regulating the brassinosteroid signaling homeostasis to regulate panicle architecture via a negative regulatory feedback loop (Deveshwar et al., 2020). It has been found that a *zinc-finger* (DROUGHT AND SALT TOLERANCE (*DST*)) negatively regulates Cytokinin accumulation in the reproductive meristem by regulating *OsCKX2* gene expression in rice. *OsCKX2* expression positively regulates Cytokinin degradation and negatively regulates panicle branching (Li et al., 2013). *OsCKX2* gene expression is decreased in young panicle mutants of the *kelch-repeat* containing F-Box protein (encoded by Larger Panicle (LP)/Erect Panicle 3 (EP3)) (Li et al., 2011; Piao et al., 2009). LP/EP3 Mutants (*ubiquitin ligase*) showed a significant increase in the number of secondary branches in the rice panicles (Li et al., 2011).

5. Conclusion

We have assessed the genetic basis of traits associated with panicle architecture using a panel of 158 rice accessions. GWAS and post-GWAS analyses, including comparative RNA-seq profiles between panicle and stem, construction of a protein-protein interaction network and haplotype analyses, identified several novel candidate genes associated with panicle traits that affect its final shape and architecture. A literature review showed that some of the genes we identified in our GWAS analyses have already been reported in the literature. Likewise, our RNA-seq data analysis validated our findings by pinpointing several genes with previous evidence for involvement in panicle formation. However, the identified genes need to be functionally characterized before they can be used in future rice breeding programs.

Author contributions

Masoumeh Kordi conducted the research as her PhD dissertation and drafted the initial manuscript. Naser Farrokhi and Asadollah Ahmadi-khah proposed the research idea, supervised the research, conducted analyses, and edited the manuscript. Abbas Saidi, Mehdi Jahanfar and Pär K. Ingvarsson read and edited the text and contributed to the discussion.

Funding

The research received no funding. Shahid Beheshti University provided the infrastructure for the research.

CRediT authorship contribution statement

Masoumeh Kordi: Writing – original draft, Formal analysis. **Pär Ingvarsson:** Writing – review & editing, Methodology. **Abbas Saidi:** Writing – review & editing, Supervision, Resources, Methodology. **Naser Farrokhi:** Writing – review & editing, Supervision, Resources, Methodology, Conceptualization. **Asadollah Ahmadi-khah:** Writing – review & editing, Supervision, Project administration, Conceptualization. **Mehdi Jahanfar:** Writing – review & editing, Supervision, Resources, Methodology.

Declaration of Competing Interest

All authors confirm that the article is the author's original work. The authors declare that they do not have any conflict of interest. This manuscript has not been submitted for publication elsewhere. All authors listed have contributed notably, read the manuscript, and agreed to its submission to Plant Science. On behalf of co-authors, the corresponding authors takes full responsibility for the submission.

Acknowledgments

We are grateful for the support of Shahid Beheshti University for providing the infrastructure and Ahwaz Agricultural Research Center for planting the rice accessions.

Sites & Software

USDA website: <https://www.ars.usda.gov/southeast-area/stuttgart-r-ar/dale-bumpers-national-rice-research-center/docs/rice-diversity-panel-1-rdp1/>
 rpart: <https://cran.r-project.org/web/packages/rpart/index.html>
 Gramene portal: <http://gramene.org>
 rMVP: <https://cran.r-project.org/web/packages/rMVP/index.html>
 Rice RNA-seq Database: <http://ipf.sustech.edu.cn/pub/ricerna/>
 Limma: <https://cran.r-project.org/web/packages/limma/index.html>
 edgeR: <https://www.bioconductor.org/packages//2.7/bioc/html/edgeR.html>
 tidyverse: <https://cran.r-project.org/web/packages/tidyverse/index.html>
 ggrepel: <https://cran.r-project.org/web/packages/ggrepel/index.html>
 STRING: <https://string-db.org/>
 PANTHER: <https://www.pantherdb.org/geneListAnalysis.do>
 FRGEpistasis: <https://bioconductor.uib.no/packages/release/bioc/html/FRGEpistasis.html>

Appendix A. Supporting information

Supplementary data associated with this article can be found in the online version at [doi:10.1016/j.plantsci.2024.112382](https://doi.org/10.1016/j.plantsci.2024.112382).

Data availability

Data will be made available on request.

References

- H. Adam, et al., Genomic introgressions from African rice (*Oryza glaberrima*) in Asian rice (*O. sativa*) lead to the identification of key QTLs for panicle architecture, *BMC Genom.* 24 (2023) 587.
- A. Agata, et al., Diverse panicle architecture results from various combinations of Pr15/GA20ox4 and Pbl6/APO1 alleles, *Commun. Biol.* 3 (2020) 302.
- A.A. Ajadi, et al., Cyclin-dependent kinase inhibitors KRP1 and KRP2 are involved in grain filling and seed germination in rice (*Oryza sativa* L.), *Int. J. Mol. Sci.* 21 (2019) 245.
- K.D. Aloryi, et al., A meta-quantitative trait loci analysis identified consensus genomic regions and candidate genes associated with grain yield in rice, *Front. Plant Sci.* 13 (2022) 1035851.
- F. Al-Tam, et al., P-TRAP: a panicle trait phenotyping tool, *BMC Plant Biol.* 13 (2013) 1–14.
- G.A. Auge, S. Penfield, K. Donohue, Pleiotropy in developmental regulation by flowering-pathway genes: is it an evolutionary constraint? *N. Phytol.* 224 (2019) 55–70.
- S. Bai, et al., Dissection of the genetic basis of rice panicle architecture using a genome-wide association study, *Rice (N. Y.)* 14 (2021a) 77.
- S. Bai, et al., Dissection of the genetic basis of rice panicle architecture using a genome-wide association study, *Rice (N. Y.)* 14 (2021b) 77.
- A. Batool, et al., **Harnessing the role of genes involved in plant architectural changes, Plant Growth Regul.** (2023), <https://doi.org/10.1007/s10725-023-00961-0>.
- J. Chebib, F. Guillaume, Pleiotropy or linkage? Their relative contributions to the genetic correlation of quantitative traits and detection by multitrait GWA studies, *iyab159*, *Genetics* 219 (2021), iyab159.
- K. Chen, et al., Genetic and molecular factors determining grain weight in rice, *Front. Plant Sci.* 12 (2021) 605799.
- J. Chen, et al., Pangenome analysis reveals genomic variations associated with domestication traits in broomcorn millet, *Nat. Genet.* 55 (2023) 2243–2254.
- M.J. Christoffers, Chapter 7 - Weed Population Genetics, in: R.L. Zimdahl (Ed.), *Fundamentals of Weed Science (Fifth Edition)*, Academic Press, 2018, pp. 179–208.
- Y. Chun, et al., Genetic and molecular pathways controlling rice inflorescence architecture, *Front. Plant Sci.* 13 (2022) 1010138.
- P. Deveshwar, A. Prusty, S. Sharma, A.K. Tyagi, Phytohormone-mediated molecular mechanisms involving multiple genes and QTL govern grain number in rice, *Front. Genet.* 11 (2020) 586462.
- H. Du, et al., Integrative regulation of drought escape through ABA-dependent and independent pathways in rice, *Mol. Plant* 11 (2018) 584–597.
- P. Duan, et al., SMALL GRAIN 1, which encodes a mitogen-activated protein kinase kinase 4, influences grain size in rice, *Plant J.* 77 (2014) 547–557.
- J. Duan, et al., Strigolactone promotes cytokinin degradation through transcriptional activation of CYTOKININ OXIDASE/DEHYDROGENASE 9 in rice, *Proc. Natl. Acad. Sci. U. S. A.* 116 (2019a) 14319–14324.
- E. Duan, et al., OsSH11 regulates plant architecture through modulating the transcriptional activity of IPA1 in rice, *Plant Cell* 31 (2019b) 1026–1042.
- N. Fang, et al., SMALL GRAIN 11 controls grain size, grain number and grain yield in rice, *Rice* 9 (1) (2016) 64 (New York, N.Y.).
- J. Fang, et al., Reduction of ATPase activity in the rice kinesin protein Stemless Dwarf 1 inhibits cell division and organ development, *Plant J.* 96 (2018) 620–634.
- J. Gui, C. Liu, J. Shen, L. Li, Grain setting defect1, encoding a remorin protein, affects the grain setting in rice through regulating plasmodesmal conductance, *Plant Physiol.* 166 (2014) 1463–1478.
- M. Guo, et al., Clustered spikelets 4, encoding a putative cytochrome P450 protein CYP724B1, is essential for rice panicle development, *Chin. Sci. Bull.* 59 (2014) 4050–4059.
- T. Guo, et al., GRAIN SIZE AND NUMBER1 negatively regulates the OsMKKK10-OsMKK4-OsMPK6 cascade to coordinate the trade-off between grain number per panicle and grain size in rice, *Plant Cell* 30 (4) (2018) 871–888.
- T. Guo, et al., Optimization of rice panicle architecture by specifically suppressing ligand–receptor pairs, *Nat. Commun.* 14 (2023) 1640.
- Y. Han, et al., Cytokinin pathway mediates APETALA1 function in the establishment of determinate floral meristems in Arabidopsis, *Proc. Natl. Acad. Sci. U. S. A.* 111 (2014) 6840–6845.
- S.H. Han, et al., Rice FLAVIN-BINDING, KELCH REPEAT, F-BOX 1 (OsFKF1) promotes flowering independent of photoperiod: OsFKF1 role in rice flowering, *Plant Cell Environ.* 38 (12) (2015) 2527–2540.
- S. Hao, et al., Genome-wide association study reveals the genetic basis of five quality traits in Chinese wheat, *Sci. Rep.* 13 (2022) 835306.
- T.W. Harrop, et al., A set of AP2-like genes is associated with inflorescence branching and architecture in domesticated rice, *J. Exp. Bot.* 70 (2019) 5617–5629.
- Z. Hu, et al., A Kelch motif-containing serine/threonine protein phosphatase determines the large grain QTL trait in rice, *J. Integr. Plant Biol.* 54 (2012) 979–990.
- L. Huang, et al., The LARGE2-APO1/APO2 regulatory module controls panicle size and grain number in rice, *Plant Cell* 33 (2021) 1212–1228.
- T. Imaizumi, et al., FKFI F-box protein mediates cyclic degradation of a repressor of CONSTANS in Arabidopsis, *Science* 309 (5732) (2005) 293–297 (New York, N.Y.).
- G. Jiang, et al., Regulation of inflorescence branch development in rice through a novel pathway involving the pentatricopeptide repeat protein sped1-D, *Genetics* 197 (2014) 1395–1407.
- S. Ke, et al., Genome-wide transcriptome profiling provides insights into panicle development of rice (*Oryza sativa* L.), *Gene* 675 (2018) 285–300.
- G.N. Khong, et al., A cluster of Ankyrin and Ankyrin-TPR repeat genes is associated with panicle branching diversity in rice, *PLoS Genet* 17 (2021) e1009594.
- K. Kitagawa, et al., A novel kinesin 13 protein regulating rice seed length, *Plant Cell Physiol.* 51 (2010) 1315–1329.
- Y. Kwon, et al., OsREL2, a rice TOPLESS homolog functions in axillary meristem development in rice inflorescence, *Plant Biotechnol. Rep.* 6 (2012) 213–224.
- M. Li, et al., Mutations in the F-box gene LARGER PANICLE improve the panicle architecture and enhance the grain yield in rice, *Plant Biotechnol. J.* 9 (2011) 1002–1013.
- S. Li, et al., Rice zinc finger protein DST enhances grain production through controlling Gn1a/OsCKX2 expression, *Proc. Natl. Acad. Sci. USA* 110 (2013) 3167–3172.
- Y. Li, et al., Panicle Morphology Mutant 1 (PMM1) determines the inflorescence architecture of rice by controlling brassinosteroid biosynthesis, *BMC Plant Biol.* 18 (2018) 1–13.
- L. Li, et al., Genome-wide association study reveals genomic regions controlling root and shoot traits at late growth stages in wheat, *Ann. Bot.* 124 (2019) 993–1006.
- Y.-F. Li, et al., MULTI-FLORET SPIKELET 2, a MYB transcription factor, determines spikelet meristem fate and floral organ identity in rice, *Plant Physiol.* 184 (2020) 988–1003.
- G. Li, et al., Detection of QTLs for panicle-related traits using an indica × japonica recombinant inbred line population in rice, *PeerJ* 9 (2021a) e12504.
- M. Li, et al., VPB1 encoding BELL-like homeodomain protein is involved in rice panicle architecture, *Int. J. Mol. Sci.* 22 (2021b) 7909.
- G. Li, et al., RGN1 controls grain number and shapes panicle architecture in rice, *Plant Biotechnol. J.* 20 (2022a) 158–167.
- P. Li, et al., Genes and their molecular functions determining seed structure, components, and quality of rice, *Rice* 15 (2022b) 18.
- C. Liang, et al., OsNAP connects abscisic acid and leaf senescence by fine-tuning abscisic acid biosynthesis and directly targeting senescence-associated genes in rice, *Proc. Natl. Acad. Sci. U. S. A.* 111 (2014) 10013–10018.
- H. Liu, et al., Dry direct-seeded rice as an alternative to transplanted-flooded rice in Central China, *Agron. Sustain. Dev.* 35 (2015) 285–294.
- X. Liu, et al., Iterative usage of fixed and random effect models for powerful and efficient genome-wide association studies, *PLoS Genet* 12 (2016) e1005767.
- Q. Lu, et al., Genetic variation and association mapping for 12 agronomic traits in indica rice, *BMC Genom.* 16 (2015) 1–17.
- A. Luo, et al., EU11, encoding a putative cytochrome P450 monooxygenase, regulates internode elongation by modulating gibberellin responses in rice, *Plant Cell Physiol.* 47 (2006) 181–191.
- J. Luo, et al., An-1 encodes a basic helix-loop-helix protein that regulates awn development, grain size, and grain number in rice, *Plant Cell* 25 (2013) 3360–3376.
- Z. Luo, et al., Genome-wide association study (GWAS) of leaf cuticular wax components in *Camelina sativa* identifies genetic loci related to intracellular wax transport, *BMC Plant Biol.* 19 (2019) 1–17.
- A.-M. Luong, PhD thesis, Université Montpellier, Impact AP2/ERF Transcr. Factors rice panicle Struct. Evol. (2019).
- Y. Lv, et al., BOST1 is a basic helix-loop-helix transcription factor involved in regulating panicle development in rice, *Front. Plant Sci.* 14 (2023) 1162828.
- L. Ming, et al., Transcriptome-wide association analyses reveal the impact of regulatory variants on rice panicle architecture and causal gene regulatory networks, *Nat. Commun.* 14 (2023) 7501.
- A. Muhammad, et al., Uncovering genomic regions controlling plant architectural traits in hexaploid wheat using different GWAS models, *BMC Plant Biol.* 11 (2021) 6767.
- R.B.S. Nabi, et al., Functional insight of nitric-oxide induced DUF genes in Arabidopsis thaliana, *Front. Plant Sci.* 11 (2020) 529438.
- H. Nakagawa, et al., Short grain1 decreases organ elongation and brassinosteroid response in rice, *Plant Physiol.* 158 (2012) 1208–1219.
- S. Narawatthana, Y. Phansenee, B.-O. Thammasamison, P. Vejchasarn, Multi-model genome-wide association studies of leaf anatomical traits and vein architecture in rice, *Front. Plant Sci.* 14 (2023) 1107718.
- F. Ntakirutimana, et al., **Genome-wide association analysis identifies natural allelic variants associated with panicle architecture variation in African rice, *Oryza glaberrima* Steud, G3 (Bethesda) (2023), <https://doi.org/10.1093/g3journal/jkad174>.**
- S.P. Ojolo, et al., Regulation of plant growth and development: A review from a chromatin remodeling perspective, *Front. Plant Sci.* 9 (2018) 1232.
- R. Panahabadi, et al., Genome-wide association mapping of mixed linkage (1, 3; 1, 4)-β-glucan and starch contents in rice whole grain, *Front. Plant Sci.* 12 (2021a) 665745.
- R. Panahabadi, et al., Genome-wide association study (GWAS) of seed germination-related traits in rice and identification of candidate genes, *BMC Plant Biol.* 21 (2021b) 1–13.
- E.A. Pasion, et al., OsTPR boosts the superior grains through increase in upper secondary rachis branches without incurring a grain quality penalty, *Plant Biotechnol. J.* 19 (2021) 1396–1411.
- R. Piao, et al., Map-based cloning of the ERECT PANICLE 3 gene in rice, *Theor. Appl. Genet.* 119 (2009) 1497–1506.
- W. Qian, et al., Novel rice mutants overexpressing the brassinosteroid catabolic gene CYP73A4A, *Plant Mol. Biol.* 93 (1–2) (2017) 197–208.
- Q. Ran, et al., SRG1, encoding a kinesin-4 protein, is an important factor for determining grain shape in rice, *Rice Sci.* 25 (2018) 297–307.
- M.A.R. Rashid, M. Sajjad, A. Gul, Y. Zhao, Genomic selection and characterization in cereals, *Front. Genet.* 13 (2023) 1092095.
- C. Rong, et al., Purine permease (PUP) family gene PUP11 positively regulates the rice seed setting rate by influencing seed development, *Plant Cell Rep.* 43 (2024) 112.
- B. Sahoo, et al., A comprehensive genome-wide investigation of the Cytochrome 71 (OsCYP71) gene family: revealing the impact of promoter and gene variants (Ser33Leu) of OsCYP71P6 on yield-related traits in indica rice (*Oryza sativa* L.), *Plants* 12 (2023) 3035.

- T. Sakamoto, et al., Erect leaves caused by brassinosteroid deficiency increase biomass production and grain yield in rice, *Nat. Biotechnol.* 24 (2006) 105–109.
- H. Seo, et al., The rice basic helix-loop-helix 79 (OsHLH079) determines leaf angle and grain shape, *Int. J. Mol. Sci.* 21 (2020) 2090.
- C. Shi, et al., Ubiquitin specific protease 15 has an important role in regulating grain width and size in rice, *Plant Physiol.* 180 (2019) 381–391.
- B. Shi, T. Vernoux, Patterning at the shoot apical meristem and phyllotaxis, *Curr. Top. Dev. Biol.* 131 (2019) 81–107.
- G. Singh, et al., 2Gs and plant architecture: breaking grain yield ceiling through breeding approaches for next wave of revolution in rice (*Oryza sativa* L.), *Crit. Rev. Biotechnol.* 44 (2024) 139–162.
- P. Sinha, et al., Fine mapping and sequence analysis reveal a promising candidate gene encoding a novel NB-ARC domain derived from wild rice (*Oryza officinalis*) that confers bacterial blight resistance, *Front. Plant Sci.* 14 (2023) 1173063.
- C. Su, et al., Stabilization of membrane topologies by proteinaceous remorin scaffolds, *Nat. Commun.* 14 (2023) 323.
- W. Sun, et al., Ustilaginoida virens: Insights into an emerging rice pathogen, *Annu. Rev. Phytopathol.* 58 (2020) 363–385.
- K.N. Ta, et al., A genome-wide association study using a Vietnamese landrace panel of rice (*Oryza sativa*) reveals new QTLs controlling panicle morphological traits, *BMC Plant Biol.* 18 (2018) 1–15.
- D. Tadesse, et al., Sorghum SbGhd7 is a major regulator of floral transition and directly represses genes crucial for flowering activation, *New Phytol.* 242 (2024) 786–796.
- C.-Y. Teh, et al., Association analysis of rice grain traits with single nucleotide polymorphisms in a Brassinosteroid-insensitive 1 (BR1)-associated receptor kinase 1-like gene, *Plant Gene* 19 (2019) 100188.
- X. Tong, et al., Notched belly grain 4, a novel allele of dwarf 11, regulates grain shape and seed germination in rice (*Oryza sativa* L.), *Int. J. Mol. Sci.* 19 (2018) 4069.
- M. Ueguchi-Tanaka, et al., GIBBERELLIN INSENSITIVE DWARF1 encodes a soluble receptor for gibberellin, *Nature* 437 (2005) 693–698.
- L. Wang, et al., OsLIC, a novel CCH-type zinc finger protein with transcription activation, mediates rice architecture via brassinosteroids signaling, *PLoS One* 3 (2008) e3521.
- Y. Wang, et al., Nanobubbles promote nutrient utilization and plant growth in rice by upregulating nutrient uptake genes and stimulating growth hormone production, *J. Agric. Food Chem.* 800 (2021) 149627.
- X. Weng, et al., Grain number, plant height, and heading date7 is a central regulator of growth, development, and stress response, *Plant Physiol.* 164 (2014) 735–747.
- S.S. Wimalagunasekara, J.W. Weeraman, S. Tirimanne, P.C. Fernando, Protein-protein interaction (PPI) network analysis reveals important hub proteins and sub-network modules for root development in rice (*Oryza sativa*), *J. Genet. Eng. Biotechnol.* 21 (2023) 69.
- T. Wu, et al., Gene SGL, encoding a kinesin-like protein with transactivation activity, is involved in grain length and plant height in rice, *Plant Cell Rep.* 33 (2014) 235–244.
- Q. Wu, et al., Overexpression of *OsDof12* affects plant architecture in rice (*Oryza sativa* L.), *Front. Plant Sci.* 6 (2015) 833.
- Y. Wu, et al., Clustered primary branch 1, a new allele of DWARF 11, controls panicle architecture and seed size in rice, *Plant Biotechnol. J.* 14 (2016) 377–386.
- Y. Wu, et al., Deletions linked to PROG1 gene participate in plant architecture domestication in Asian and African rice, *Nat. Commun.* 9 (1) (2018) 4157.
- J. Wu, et al., The OsNLP3/4-OsRFLmodule regulates nitrogen-promoted panicle architecture in rice, *New Phytol.* 240 (6) (2023) 2404–2418.
- H. Xiao, et al., STAMENLESS 1, encoding a single C2H2 zinc finger protein, regulates floral organ identity in rice, *Plant J.* 59 (2009) 789–801.
- C. Xie, et al., Phytochrome-interacting factor-like protein OsPIL15 integrates light and gravitropism to regulate tiller angle in rice, *Planta* 250 (2019) 105–114.
- Y. Xie, et al., Arabidopsis FHY3 and FAR1 integrate light and strigolactone signaling to regulate branching, *Nat. Commun.* 11 (1) (2020) 1955.
- X. Xie, et al., Genome-wide association study of QTLs conferring resistance to bacterial leaf streak in rice, *BMC Genet* 10 (2021) 2039.
- X. Xu, et al., Quantitative trait loci identification and genetic diversity analysis of panicle structure and grain shape in rice, *Plant Growth Regul.* 90 (1) (2020) 89–100.
- D. Yan, et al., BEAK-SHAPED GRAIN 1/TRIANGULAR HULL 1, a DUF640 gene, is associated with grain shape, size and weight in rice, *Sci. China Life Sci.* 56 (2013) 275–283.
- P. Yan, et al., A new RING finger protein, PLANT ARCHITECTURE and GRAIN NUMBER 1, affects plant architecture and grain yield in rice, *Int. J. Mol. Sci.* 23 (2022) 824.
- X. Yang, et al., Overexpression of OsHLH107, a member of the basic helix-loop-helix transcription factor family, enhances grain size in rice (*Oryza sativa* L.), *Rice* 11 (2018) 1–12.
- X. Yang, et al., OsTTG1, a WD40 repeat gene, regulates anthocyanin biosynthesis in rice, *Plant J.* 107 (2021) 198–214.
- Y. Yao, et al., Control of rice ratooning ability by a nucleoredoxin that inhibits histidine kinase dimerization to attenuate cytokinin signaling in axillary buds, *J. Exp. Bot.* 16 (2023) 1911–1926.
- Z. Ye, et al., Genome-wide identification and expression analysis of kinesin family in barley (*Hordeum vulgare*), *Genes* 13 (2022) 2376.
- A. Yoshida, et al., ABERRANT SPIKELET AND PANICLE1, encoding a TOPLESS-related transcriptional co-repressor, is involved in the regulation of meristem fate in rice, *Plant J.* 70 (2012) 327–339.
- X. Zha, et al., Over-expression of the rice LRK1 gene improves quantitative yield components, *Plant Biotechnol. J.* 7 (2009) 611–620.
- Z. Zhang, et al., Mixed linear model approach adapted for genome-wide association studies, *Nat. Genet.* 42 (2010) 355–360.
- Z. Zhang, et al., Proteomic and phosphoproteomic determination of ABA's effects on grain-filling of *Oryza sativa* L. inferior spikelets, *J. Proteom.* 185 (2012a) 259–273.
- J.-W. Zhang, et al., OsGLU3, a putative membrane-bound endo-1, 4-beta-glucanase, is required for root cell elongation and division in rice (*Oryza sativa* L.), *Mol. Plant* 5 (2012a) 176–186.
- X. Zhang, et al., Rare allele of OsPPKL1 associated with grain length causes extra-large grain and a significant yield increase in rice, *Proc. Natl. Acad. Sci. U. S. A.* 109 (2012b) 21534–21539.
- Y.J. Zhang, et al., The transcription factor OsGATA6 regulates rice heading date and grain number per panicle, *J. Exp. Bot.* 73 (2022) 6133–6149.
- C. Zhang, M.-Y. Bai, K. Chong, Brassinosteroid-mediated regulation of agronomic traits in rice, *Plant Cell Rep.* 33 (2014) 683–696.
- X. Zhang, J. Wang, J. Huang, H. Lan, C. Wang, C. Yin, SB1 encoding RING-like zinc-finger protein regulates branch development as a transcription repressor, *Rice Sci.* 28 (2021) 243–256.
- K. Zhao, et al., Genome-wide association mapping reveals a rich genetic architecture of complex traits in *Oryza sativa*, *Nat. Commun.* 2 (2011) 467.
- L. Zhao, et al., PAY 1 improves plant architecture and enhances grain yield in rice, *Plant J.* 83 (2015) 528–536.
- X. Zhao, et al., Morphological, transcriptomic and metabolomic analyses of *Sophora davidii* mutants for plant height, *BMC Plant Biol.* 22 (1) (2022) 144.
- H. Zheng, et al., Identification of candidate genes for panicle length in *Oryza sativa* L. ssp. japonica via genome-wide association study and linkage mapping, *Euphytica* 218 (2022) 16.
- H. Zhong, et al., Uncovering the genetic mechanisms regulating panicle traits in rice with dissection of a single multiple mutant population, *Front. Plant Sci.* 12 (2021) 730785.
- Y. Zhou, et al., GNS4, a novel allele of DWARF11, regulates grain number and grain size in a high-yield rice variety, *Rice* 10 (2017) 1–11.
- L. Zhu, et al., Ubiquitinome profiling reveals the landscape of ubiquitination regulation in rice young panicles, *Genom. Proteom. Bioinforma.* 18 (2020) 305–320.
- W. Zhu, et al., Rice SEPALLATA genes OsMADS5 and OsMADS34 cooperate to limit inflorescence branching by repressing the TERMINAL FLOWER1-like gene RCN4, *N. Phytol.* 233 (2022) 1682–1700.
- H. Zhuang, et al., NONSTOP GLUMES1 encodes a C2H2 zinc finger protein that regulates spikelet development in rice, *Plant Cell* 32 (2020) 392–413.
- R.L. Zimdahl, *Fundamentals of Weed Science*, Elsevier Academic Press, 2024.
- X. Zou, et al., Over-expression of an S-domain receptor-like kinase extracellular domain improves panicle architecture and grain yield in rice, *J. Exp. Bot.* 66 (2015) 7197–7209.